Journal of Engineering Mathematics 22: 267–284 (1988)

The cubic autocatalator: The influence of the quadratic autocatalytic and the uncatalysed reactions

B.F. GRAY,[1] M.J. ROBERTS[1] and J.H. MERKIN[2]
[1] *School of Chemistry, Macquarie University, Sydney, New South Wales 2109, Australia;*
[2] *School of Mathematics, University of Leeds, Leeds, LS2 9JT, UK*

Received 9 February 1988; accepted 28 March 1988

Abstract. The proptotype chemical reaction scheme, the cubic autocatalator, A + 2B → 3B; B → C is taken in a closed system, with A formed from the precursor P by the simple step P → A. The pooled chemical approximation is invoked whereby the concentration of P can be assumed to remain constant throughout. The effects of allowing the quadratic autocatalytic reaction A + B → 2B and the uncatalysed reaction A → B in the scheme are considered in detail. The full scheme is described by the non-dimensional parameters μ (measuring the reaction rate of the initiation step) and s and r (measuring the reaction rates of the quadratic autocatalytic and the uncatalysed steps respectively). It is shown, provided only that r or s (or both) are non-zero, no matter how small, the solution remains bounded for all (positive) values of μ, whereas with $r = s = 0$ the solution is bounded only for $\mu > \mu_0$ ($\mu_0 = 0.900\,32$). It is shown that with $r = 0$ and $s \neq 0$ the governing equations have a Hopf bifurcation at $\mu = 1 - s$ producing a stable limit cycle which exists for all μ in $0 < \mu < 1 - s$. The behaviour of these limit cycles as $\mu \to 0$ is also discussed.

1. Introduction

In recent years several prototype isothermal chemical reaction schemes have been proposed in an attempt to model the oscillatory behaviour observed in certain chemical reactions. The simplest and, arguably, the most chemically viable, is the cubic autocatalator introduced originally by Gray and Scott [1]. This scheme is based on a cubic autocatalytic step and the simple first-order decay of the catalyst, namely

$$\mathrm{A} + 2\mathrm{B} \to 3\mathrm{B} \qquad \text{rate } k_1 ab^2, \tag{1}$$

$$\mathrm{B} \to \mathrm{C} \qquad \text{rate } k_2 b. \tag{2}$$

(Where a and b are the concentrations of the reactants A and B and k_1 and k_2 are rate constants). The basic scheme given by (1) and (2) has been studied extensively for an open system (the C.S.T.R.), see, for example, recent papers by Gray and Scott [2], D'Anna et al. [3], and Gray and Roberts [4], where it has been shown to exhibit a complex pattern of behaviour.

More recently this scheme has been used to model reactions in closed systems with now the inflow of fresh reactant A in the C.S.T.R. replaced by the production of A by the slow first-order decay of a precursor P

$$\mathrm{P} \to \mathrm{A} \qquad \text{rate } k_0 p. \tag{3}$$

Consequent on this is the assumption that the reactant P is present in large excess (relative to the intermediates A and B). In such circumstances it is usual to invoke the "pooled

chemical approximation" and make the further assumption whereby the concentration of P is taken to be constant (at its initial value p_0) throughout the reaction.

A major criticism of this scheme (and other similar schemes) is that they are selective in which reaction steps are considered. In this case just the termolecular step (1) is included whereas, in reality, both the uncatalysed reaction

$$\mathrm{A} \rightarrow \mathrm{B} \qquad \text{rate } k_3 a \tag{4}$$

and the quadratic autocatalytic reaction

$$\mathrm{A} + \mathrm{B} \rightarrow 2\mathrm{B} \qquad \text{rate } k_4 ab \tag{5}$$

will also be present. These last two reaction steps are assumed to be slow compared with the basic step (1) but even so they can have a considerable effect in the overall behaviour. It was shown, [5], that the inclusion of the uncatalysed reaction (4) completely changes the oscillatory behaviour, and as it is the possibility of obtaining oscillations in these schemes that is of predominant interest, it is important to examine the influence of the extra steps (4) and (5) on the basic scheme (1), (2) and (3).

Following [5] and [6] the non-dimensional equations governing the full reaction scheme (1)–(5) are

$$\frac{\mathrm{d}x}{\mathrm{d}t} = \mu - xy^2 - rx - sxy, \tag{6(i)}$$

$$\frac{\mathrm{d}y}{\mathrm{d}t} = xy^2 - y + rx + sxy, \tag{6(ii)}$$

where $x = (k_1/k_2)^{1/2} a$, $y = (k_1/k_2)^{1/2} b$ are the non-dimensional concentrations of A and B, $t = k_2 \bar{t}$ ($\bar{t}$ is time) and $\mu = (k_1/k_2)\, k_0 p_0/k_2$ is a constant. r and s are respectively constants describing the relative importance of the uncatalysed step (4) and the quadratic autocatalytic step (5) given by $r = k_3/k_2$ and $s = (k_4/(k_2 k_1)^{1/2}$, (note that in [5] the reciprocal of r was used).

The basic scheme (with $r = s = 0$) was considered in some detail in [6], where it was shown that there is one (finite) stationary state $x_s = \mu^{-1}$, $y_s = \mu$ which is stable for $\mu \geqslant 1$. The change in stability at $\mu = 1$ gives rise (through a Hopf bifurcation) to a stable limit cycle which exists for $\mu_c < \mu < 1$ with $\mu_c = 0.900\,32$. For $0 < \mu < \mu_c$ the solution becomes unbounded, with $x \sim \mu t$, $y \rightarrow 0$ as $t \rightarrow \infty$. The effect of including the uncatalysed reaction ($r \neq 0$) was considered in [5] where it was shown that the effect of including this extra term was to introduce an extra Hopf bifurcation point (provided $r < \frac{1}{8}$) there now being two values of μ at which Hopf bifurcation occurs (μ_0 and μ_1 (say) with $0 < \mu_0 < \mu_1 < 1$). Further it was shown that, provided *only* that $r \neq 0$, i.e., r can be arbitrarily small, a stable limit cycle existed (i.e., the solution remained bounded and oscillatory) for all μ in the range $\mu_0 < \mu < \mu_1$. When $r > \frac{1}{8}$ the stationary state remained stable for all μ.

The purpose of this paper is to consider the full reaction scheme (6) in which the terms involving both r and s are included. We find that there is a range of values of r and s

($r \neq 0$, $s \neq 0$) such that for a given value of r and s there are two values of μ at which a Hopf bifurcation takes place, with a stable limit cycle existing for all μ between them. So in this respect the inclusion of the extra quadratic step (5) does not radically alter the behaviour seen with just the uncatalysed step included. However, when we consider the case with only s non-zero (i.e., equations (6) with $r = 0$) we find a different situation to that which holds when only the uncatalysed step (4) is included, as described in [5]. Here there is just one value of $\mu = \mu_0$ at which a Hopf bifurcation occurs ($\mu_0 = 1 - s$) with a stable limit cycle existing for all μ in the open interval $0 < \mu < \mu_0$. To show that this is the case it is necessary to consider the phase plane at infinity, as was needed in [6] for the basic scheme. A further consideration of these limit cycles shows that, though their amplitudes remain finite, the periods become infinite (proportional to μ^{-1}) as $\mu \to 0$. Then we can conclude that the basic scheme is also structurally unstable with respect to the inclusion of the quadratic step, i.e., the solution remains bounded for all μ provided only that $s \neq 0$.

2. Phase-plane analysis for the general case ($r \neq 0$, $s \neq 0$)

Equations (6) possess the single (finite) stationary state

$$x_s = \frac{\mu}{\mu^2 + s\mu + r}, \qquad y_s = \mu. \tag{7}$$

The stability of (x_s, y_s) is determined from the equation for the eigenvalues λ,

$$\lambda^2 + (y_s^2 + sy_s + r + 1 - 2x_s y_s - sx_s)\lambda + y_s^2 + sy_s + r = 0. \tag{8}$$

Equation (8) is obtained by linearising equations (6) about (x_s, y_s) and then looking for a solution proportional to $e^{\lambda t}$. The constant term in (8) is always positive and hence there will be a Hopf bifurcation when the coefficient of λ is zero. On using (7), we find that the values of μ at which Hopf bifurcations occur are given by the positive solutions of the quartic equation

$$f(\mu) \equiv \mu^4 + 2s\mu^3 + (s^2 + 2r - 1)\mu^2 + 2rs\mu + r + r^2 = 0. \tag{9}$$

Equation (9) reduces to that given in [5] when $s = 0$. Since $f(0) > 0, f \sim \mu^4$ for $\mu \gg 1$ and there can be at most two changes in sign of the coefficients, there will be either two or no positive roots of equation (9). Also, clearly a necessary condition for a positive solution is that

$$s^2 + 2r - 1 < 0, \tag{10}$$

so that there must be a limited range of values of r and s over which Hopf bifurcations can occur. To determine this we calculate the $H2_1$ bifurcation points where the two positive roots of $f(\mu) = 0$ are co-incident. These are found by showing $f(\mu) = 0$ together with the

equation (Gray and Roberts [7])

$$\frac{df}{d\mu} = 4\mu^3 + 6s\mu^2 + 2(s^2 + 2r - 1)\mu + 2rs = 0. \tag{11}$$

μ can then be eliminated from equations (9) and (11) to give a relation between r and s.

It is much easier to proceed implicitly. From (7),

$$x_s = \frac{y_s}{y_s^2 + sy_s + r}, \tag{12}$$

from which it follows, after using (12) again to eliminate r, that

$$\frac{dy_s}{dx_s} = -\frac{y_s}{x_s(2x_s y_s + sx_s - 1)}. \tag{13}$$

Now, on the Hopf curve, $T_r = 2x_s y_s + s(x_s - y_s) - y_s^2 - r - 1 = 0$, so that, again using (12),

$$\mu = y_s = \frac{1 - sx_s}{2x_s^2 - 1}, \qquad r = \frac{(1 - sx_s)^2(x_s^2 - 1)}{(2x_s^2 - 1)^2}. \tag{14}$$

The $H2_1$ points are then found from the condition that $dT_r/dx_s = 0$, as well as $T_r = 0$, which gives

$$(2y_s + s - 2x_s)\frac{dy_s}{dx_s} + (2y_s + s) = 0. \tag{15}$$

Expression (13) is first used in (15) and then y_s eliminated using (14) giving, after some algebra the expression for s in terms of x_s:

$$s = x_s(3 - 2x_s^2). \tag{16}$$

Then using (16) in (14) we obtain finally

$$r = (x_s^2 - 1)^3 \tag{17}$$

(with $\mu = y_s = x_s(x_s^2 - 1)$).

Equations (16) and (17) give the $H2_1$ curve implicitly in terms of the parameter x_s with, since $r \geqslant 0$, $s \geqslant 0$, $1 \leqslant x_s \leqslant \sqrt{3/2}$. Alternatively, x_s can be eliminated from (16) and (17) to give the double Hopf curve directly as

$$s^2 = 1 - 3r^{1/3} + 4r. \tag{18}$$

A graph of s against r as calculated from (18) is shown in Fig. 1, where we can see that we must have the overall bounds for oscillatory solutions $s \leqslant 1$, $r \leqslant 1/8$ and that the slope of the curve becomes infinite as $r \to 0$ (and $s \to 1$).

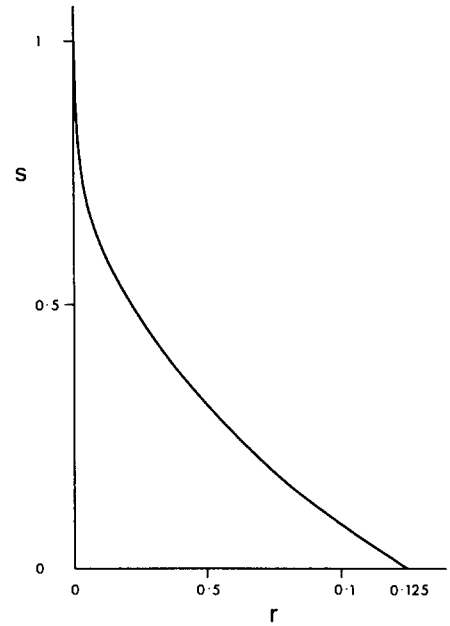

Fig. 1. The double Hopf curve as given by equation (18).

Having established the range of the parameters r and s over which Hopf bifurcations can occur, the next step is to determine the stability of the limit cycles thus produced. To do this we first put $\xi = x + y$ and $\eta = \beta y$ where $\beta = (\mu^2 + \mu s + r)^{1/2}$, with equations (6) becoming

$$\frac{d\xi}{dt} = \mu - \frac{\eta}{\beta}, \tag{19(i)}$$

$$\frac{d\eta}{dt} = \frac{1}{\beta^2}(\beta\xi - \eta)(\eta^2 + r\beta^2 + s\beta\eta) - \eta. \tag{19(ii)}$$

At bifurcation $\xi_s = (\mu/\beta^2)(1 + \beta^2)$, $\eta_s = \mu/\beta$ with μ given by equation (9). It is straightforward to check that equations (19) are in normal form and, using the result given by Guckenheimer and Holmes [8], it follows, after some calculation, that the stability is determined by the sign of

$$\mu_2 = -\tfrac{1}{8}(1 + 4r - s^2). \tag{20}$$

Using (10) we can see that $\mu_2 < 0$ for all values of r and s for which a Hopf bifurcation occurs, so that for all these values a stable limit cycle is produced surrounding the equilibrium point (x_s, y_s) whenever this is unstable.

The above argument enables us to conclude that for given values of r and s such that

$$s < \sqrt{1 - 3r^{1/3} + 4r}, \qquad s > 0, r > 0, \tag{21}$$

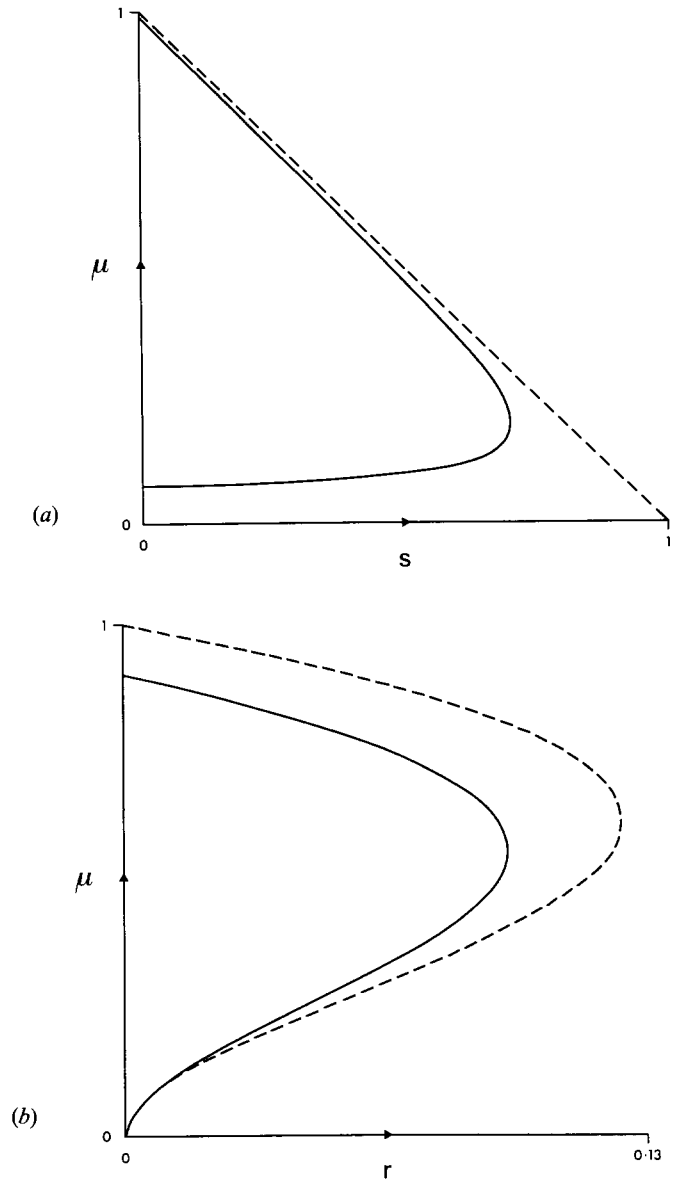

Fig. 2. Hopf bifurcation curves: (a) μ plotted against s for $r = 0.05$, (the case $r = 0$ is shown by the broken line). (b) μ plotted against r for $s = 0.1$ (the case $s = 0$ is shown by the broken line).

there are two values of μ, μ_0 and μ_1 (say) with $0 < \mu_0 < \mu_1$, at which there are Hopf functions. Furthermore, these bifurcations give rise to a stable limit cycle in $\mu > \mu_0$ and in $\mu < \mu_1$ respectively. We shall see later (from numerical solutions) that we can regard the Hopf bifurcation at $\mu = \mu_1$ as giving birth to a stable limit cycle which then exists for all μ in the interval $\mu_0 < \mu < \mu_1$ before being destroyed at $\mu = \mu_0$ by a second Hopf bifurcation. Typical graphs of values of μ at which Hopf bifurcations occur plotted against s and r are shown in Figs. 2a and 2b respectively. For r and s which do not satisfy (21), the stationary state (7) is stable and $(x, y) \to (x_s, y_s)$ as $t \to \infty$.

Finally in this section we obtain the solution of equation (9) when $r \ll 1$. One root is regular in r and it is easy to show that this is

$$\mu = (1 - s) - \frac{(3 - 2s)}{2(1 - s)^2} r + \ldots . \tag{22}$$

A balancing of terms in equation (9) shows that the second root is $O(r^{1/2})$ for r small, and in expanding in powers of $r^{1/2}$ we find that this second root is of the form

$$\mu = r^{1/2}\left(\frac{1}{(1 - s^2)^{1/2}} + \frac{(2 - s^2)s}{(1 - s^2)^2} r^{1/2} + \ldots\right). \tag{23}$$

(23) clearly shows the singular nature of this second root as $r \to 0$ and as $s \to 1$.

3. The quadratic step only ($r = 0$)

(i) phase-plane analysis

Here we consider the behaviour of equations (6) when $r = 0$. The stationary state (7) becomes $x_s = 1/(\mu + s)$, $y_s = \mu$ and equation (9) now has just the one solution

$$\mu_1 = 1 - s, \tag{24}$$

so that for $0 < s < 1$ there is just one Hopf bifurcation point $\mu = \mu_1$ which, from (20), produces a stable limit cycle in $\mu < \mu_1$. We now show that this limit cycle exists for all μ in the range $0 < \mu < \mu_1$ provided only that $s \neq 0$. This contrasts with the case when $s = 0$ where the limit cycle exists only for $\mu_c < \mu < 1$ ($\mu_c = 0.900\,32$). To do this we need to determine the phase plane at infinity.

Following Andronov et al. [9], we first write $x = 1/z$, $y = u/z$. This transformation maps the quadrant $x > 0$, $y > 0$ bijectively onto the quadrant $u > 0$, $z > 0$ in the (u, z) plane and is constructed so that as $x \to \infty$ the lines $y/x =$ constant are mapped into the lines $u =$ constant as $u \to 0^+$. So the behaviour near the "arc at infinity" $x^2 + y^2 \to \infty$ is mapped into the neighbourhood of the line $z = 0^+$ in the (u, z) plane. We can discuss the behaviour of the paths at infinity in the (x, y) plane by examining the corresponding paths in the finite (u, z) plane. (The point at infinity on the y-axis is also mapped to infinity by this transformation and this point has to be considered separately).

In terms of u and z, the reduced forms [9], of equations (6) are

$$\begin{aligned} \frac{dz}{dt} &= -z(\mu z^3 - u^2 - suz), \\ \frac{du}{dt} &= u^2 - uz^2 + suz - \mu uz^3 + u^3 + su^2 z. \end{aligned} \tag{25}$$

The only (physically acceptable) equilibrium point of equations (25) on $z = 0$ is $u = 0$ (i.e., situated at the positive "end" if the x-axis) and we need to determine the behaviour of equations (25) in the neighbourhood of $u = 0$, $z = 0$.

On $z = 0$, $\mathrm{d}z/\mathrm{d}t = 0$ and $\mathrm{d}u/\mathrm{d}t = u^2 + u^3 > 0$ while on $u = 0$, $\mathrm{d}u/\mathrm{d}t = 0$ and $\mathrm{d}z/\mathrm{d}t = -\mu z^4 < 0$. Also the vertical isocline is given by $\mu z^3 - u^2 - suz = 0$ so that (for $u \geqslant 0$)

$$u = \tfrac{1}{2}(-sz + \sqrt{s^2z^2 + 4\mu z^3}) \tag{26}$$

with $u = (\mu/s)z^2 + \ldots$ for $z \ll 1$, and on this isocline $\mathrm{d}u/\mathrm{d}t = \mu z^3 \geqslant 0$ (again for z small). Furthermore the horizontal isocline

$$u^2 + u(1 + sz) + sz - z^2 - \mu z^3 = 0 \tag{27}$$

has no solutions for u which are positive for z small, in fact $u = -(1 - sz + \ldots)$ and $u = -sz + \ldots$. So there is no horizontal isocline close to the origin in the positive part of the (u, z) plane. We can use the above information to conclude that this equilibrium point has a saddle-like behaviour near $u = 0^+$, $z = 0^+$ (and is unstable).

We next turn to the point at infinity at the positive "end" of the y-axis. To discuss the behaviour near this point we put $x = v/z$, $y = 1/z$ and consider the (v, z) plane near $v = 0$, $z = 0$. The reduced forms of equations (6) are now

$$\begin{aligned} \frac{\mathrm{d}z}{\mathrm{d}t} &= -z(v - z^2 + svz), \\ \frac{\mathrm{d}v}{\mathrm{d}t} &= \mu z^3 - v - svz - v^2 + vz^2 - sv^2z. \end{aligned} \tag{28}$$

We can see that $v = 0$, $z = 0$ is an equilibrium point of equations (28) and that on $z = 0$, $\mathrm{d}z/\mathrm{d}t = 0$, $\mathrm{d}v/\mathrm{d}t = -(v + v^2) < 0$ and on $v = 0$, $\mathrm{d}v/\mathrm{d}t = \mu z^3 > 0$, $\mathrm{d}z/\mathrm{d}t = z^4 > 0$. The vertical isocline is $v = z^2/(1 + sz) \simeq z^2$ for small z, with then $\mathrm{d}v/\mathrm{d}t = -z^2 < 0$. The horizontal isocline is given by $v = \mu z^3 + \ldots$ (with then $\mathrm{d}v/\mathrm{d}t = -z^2 < 0$). The horizontal isocline is given by $v = \mu z^3 + \ldots$ (with $\mathrm{d}z/\mathrm{d}t = z^3 + \ldots > 0$) for small z. From this we can see that close to the equilibrium point $v = 0$, $z = 0$ the picture is essentially the same as for the case when $s = 0$, described in [6]. Consequently this equilibrium point too has a saddle-like behaviour (and is unstable). In particular there is an algebraic path $y = \sqrt{\mu}x^{-1/2} - \frac{1}{2}s + \ldots$ for $x \ll 1$, $y \gg 1$ which divides the phase plane between those trajectories which enter the positive quadrant across the y-axis and those which are turned round by the saddle at the positive "end" of the y-axis.

To complete the discussion we note that, for equations (6), on $x = 0$, $\mathrm{d}x/\mathrm{d}t = \mu > 0$ and $\mathrm{d}y/\mathrm{d}t = -y < 0$ and that the axis $y = 0$ is a solution curve, so that no trajectory can leave the positive quadrant and any trajectory which enters the positive quadrant across the y-axis must remain there. Then when $\mu < 1 - s$ the (finite) equilibrium point is unstable as well as the equilibrium points at infinity, so, by an application of the Poincaré–Bendixson theorem [10] there must be at least one stable limit cycle in the positive quadrant. Further, since there is only one point of Hopf bifurcation, we can conclude that for all $\mu < 1 - s$

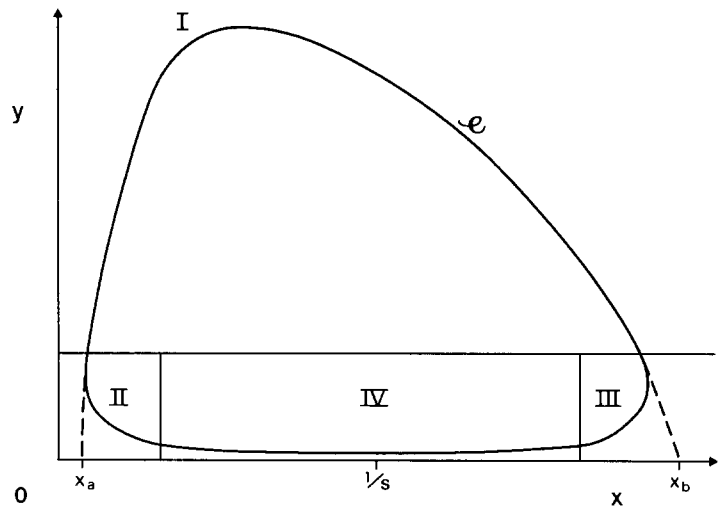

Fig. 3. Schematic picture of the limit cycle $\mathscr{C}$ as $\mu \to 0$ showing the four regions to be matched.

there is a single stable limit cycle surrounding the equilibrium point $((\mu + s)^{-1}, \mu)$ for all $\mu < 1 - s$.

We now go on to discuss the behaviour of this limit cycle was $\mu \to 0$.

(ii) limit cycle as $\mu \to 0$

To discuss the behaviour of the limit cycles of equations (6) (with $r = 0$) as $\mu \to 0$ we work in the phase plane variables (x, y) and solve for $x = x(y)$. Equations (6) can be combined to give

$$\frac{dx}{dy} = \frac{\mu - xy^2 - sxy}{xy^2 - y + sxy}. \tag{29}$$

We have seen above that any closed orbit solution of equation (29) must be entirely in the positive quadrant, and denoting such a closed curve by $\mathscr{C}$ we obtain a uniform approximation for $\mathscr{C}$ for $\mu \ll 1$. To do this we have to solve in four separate regions, a schematic picture which is shown in Fig. 3.

We start in region I where x and y are both of O(1) and expand

$$x(y; \mu) = x_0(y) + x_1(y)\mu + \ldots \tag{30}$$

where, at leading order,

$$\frac{dx_0}{dy} = \frac{x_0(s + y)}{1 - x_0(s + y)}. \tag{31}$$

The vertical isoclines of equation (31) are $x_0 = 0$ and $y = -s$, and the horizontal isocline is $x_0 = 1/(s + y)$. Also on $y = 0$, $dx_0/dy = sx_0/(1 - sx_0)$ which is positive if $x_0 < 1/s$ and negative if $x_0 < 1/s$ and negative if $x_0 > 1/s$. This enables us to deduce that there is a family

of integral curves of equation (31) which cross the x_0-axis once in $x_0 < 1/s$ and once in $x_0 > 1/s$. Take one such curve and let it cross the x_0-axis at $x_0 = x_a$ and $x_0 = x_b$, where $0 < x_a < 1/s < x_b$. Then, in I, x is given by

$$x = x_0(y) + O(\mu), \tag{32}$$

$$x_0(0) = x_a \ (x_0 < 1/s), \quad x_0(0) = x_b \quad (x_0 > 1/s). \tag{33}$$

x_a and x_b will be determined by the matching process.

Expansion (30) breaks down when y is $O(\mu)$ and this gives two further regions. Consider region II first. In II we put

$$x = x_a + \mu X, \qquad y = \mu Y \tag{34}$$

where now X and Y are both of O(1). We then expand $X(Y)$ in the form

$$X = X_0(Y) + \ldots \tag{35}$$

with, at leading order,

$$\frac{dX_0}{dY} = \frac{sx_a Y - 1}{(1 - sx_a)Y}. \tag{36}$$

Equation (36) has the solution

$$X_0 = \frac{1}{1 - sx_a}(sx_a Y - \log A_0 Y) \tag{37}$$

for some constant A_0. Then in II we have

$$x = x_a + \frac{\mu}{1 - sx_a}(sx_a Y - \log A_0 Y) + \ldots, \tag{38}$$

which matches I to leading order.

Region III is similar to region II in that y is $O(\mu)$ and $x = x_b + O(\mu)$, and by a similar argument to that for region II we find that in region III

$$x = x_b + \frac{\mu}{sx_b - 1}(\log B_0 Y - sx_b Y) + \ldots \tag{39}$$

where $Y = \mu^{-1}y$ (as before) and B_0 is a further arbitrary constant.

We then need a final region (region IV) to complete the closed curve $\mathscr{C}$ and which matches with regions II and III. Writing (38) (or equivalently (39)) in terms of the original variable y we have that $x = x_a + \{\mu/(1 - sx_a)\} \log(y/\mu) + \ldots$. This expansion breaks down (the first perturbation becomes of O(1)) when y is of $O(\mu e^{-1/\mu})$, so that in IV $y \ll \mu$. On this assumption, equation (29) becomes, approximately,

$$\frac{dx}{dy} = \frac{\mu}{(sx - 1)y}. \tag{40}$$

Equation (40) can be solved implicitly to give

$$y = C(\mu) \exp\left[\frac{1}{2\mu}\left(\sqrt{s}\, x - \frac{1}{\sqrt{s}}\right)^2\right] \tag{41}$$

where $C(\mu)$ is an arbitrary constant. On re-arranging (41) we get

$$x = \frac{1}{s} \pm \frac{1}{\sqrt{s}}\left[2\mu \log\left(\frac{y}{C(\mu)}\right)\right]^{1/2} \tag{42}$$

where the solution with the $-$ sign is to match with region II and that with the $+$ sign to region III.

On writing (42) in terms of $Y = \mu^{-1}y$, we can see that for it to match with (38) $C(\mu)$ must be of the form

$$C(\mu) = C_0 \mu\, \mathrm{e}^{-\gamma/\mu} \tag{43}$$

where C_0 and γ are both constants of O(1). Then using (43) in (42) and expanding, we get

$$x = \frac{1}{s} - \frac{\sqrt{2\gamma}}{\sqrt{s}}\left(1 + \frac{\mu}{2\gamma} \log C_0 Y + \ldots\right). \tag{44}$$

The matching between (44) and (38) then gives

$$\gamma = \frac{(1 - sx_a)^2}{2s}, \qquad C_0 = A_0, \tag{45}$$

and the solution in IV becomes

$$x = \frac{1}{s} \pm \left[2\mu \log\left(A_0 \frac{y}{\mu} \exp\left(\frac{(1 - sx_a)^2}{2s\mu}\right)\right)\right]^{1/2}, \tag{46}$$

which when expanded, now using the $+$ sign, gives

$$x = \frac{1}{s} + \frac{1 - sx_a}{s}\left(1 + \frac{\mu s}{(1 - sx_a)^2} \log (A_0 Y) + \ldots\right). \tag{47}$$

For (47) to match with the solution in region III given by (39) we must have $B_0 = A_0$ and

$$x_a + x_b = \frac{2}{s}. \tag{48}$$

This final matching closes the orbit $\mathscr{C}$.

It then remains to solve equation (31), subject to boundary conditions (33) and (48). The solution of equations (31) which satisfies $x_0(0) = x_a$ is found to be, after a little

Table 1. Values of x_a calculated by solving equation (50) for various s

s	x_a
0.999	0.930 27
0.995	0.846 71
0.99	0.785 93
0.98	0.702 58
0.95	0.546 20
0.90	0.385 18
0.85	0.274 39
0.80	0.191 60
0.75	0.128 55
0.70	0.08114
0.65	0.046 88
0.60	0.023 83
0.55	0.010 03
0.50	0.003 18
0.45	0.000 65
0.40	0.000 06

calculation,

$$x_0 = x_a \exp\left(\tfrac{1}{2}(x_0 + y + s)^2\right)\left(\exp\left(\tfrac{1}{2}(x_a + s)^2\right) + x_a \int_{x_a+s}^{x_0+y+s} e^{u^2/2}\, du\right)^{-1}. \tag{49}$$

On applying $x_0(0) = x_b$ to (49) and using condition (48) it follows that x_a (and from this x_b) is given by the root of the equation

$$F(x) \equiv \frac{\exp\left(\tfrac{1}{2}(2/s + s - x)^2\right)}{2/s - x} - \frac{\exp\left(\tfrac{1}{2}(x + s)^2\right)}{x} - \int_{x+s}^{2/s+s-x} \exp\left(\frac{u^2}{2}\right) du = 0. \tag{50}$$

It is straightforward to show that $F(x)$ is odd about $x = 1/s$ (i.e., $F(2s^{-1} - x) = -F(x)$) and that there is just one root in $0 < x < 1/s$ (the root $x = 1/s$ is the trivial solution and is not required). In general equation (50) has to be solved numerically with the results given in Table 1 for a range of s. However, we can deduce the behaviour of x_a both as $s \to 0$ and as $s \to 1$. In the former case we find that the solution has an essential singularity of the form

$$x_a = 8e^{-2}\, e^{-2/s^2} s^{-3} + \ldots \tag{51}$$

as $s \to 0$, from which it follows that x_a is very small even for quite moderate values of s (with $s = 0.4$ expression (51) gives $x_a = 6.3 \times 10^{-5}$) in line with the results given in Table 1.

As $s \to 1$ we find, after a little calculation that x_a again develops a singularity, now of the form

$$x_a = \frac{1}{s} - \left(\frac{10(1 + s)s^2}{11s^6 - 6s^4 - 1}\right)(1 - s)^{1/2} + \ldots. \tag{52}$$

The above analysis shows that the amplitude of the limit cycle remains finite as $\mu \to 0$, in fact, if we define the amplitude $A_x = x_{\max} - x_{\min}$, then

$$A_x \to 2\left(\frac{1}{s} - x_a\right) \quad \text{as} \quad \mu \to 0. \tag{53}$$

However, the solution does become singular as $\mu \to 0$ in that the period of the oscillatory response becomes infinite. It is this that we now consider.

Without loss of generality we can start in region II at $y = \mu/x_a$, $x = x_a + \{\mu/(1 - sx_a)\}$ $\{s - \log(A_0/x_a)\}$, then using (34) equation 6(ii) becomes

$$\frac{dY}{dt} = -(1 - sx_a)Y, \tag{54}$$

which has the solution

$$Y = x_a^{-1} \exp(-(1 - sx_a)t). \tag{55}$$

Putting (55) in (38) then gives

$$x = x_a + \frac{\mu}{1 - sx_a}\left(s \exp(-(1 - sx_a)t) + (1 - sx_a)t - \log\left(\frac{A_0}{x_a}\right)\right) + \ldots. \tag{56}$$

Expansion (56) breaks down when t is of O (μ^{-1}) and this puts us into region IV with independent variable now $\tau = \mu t$ (and $y \ll \mu$). Equation (6(i)) gives, at leading order just $dx/dt = 1$, so that in IV

$$x = x_a + \tau \tag{57}$$

to match with (56) for $t \gg 1$. Using this in (41) we obtain

$$y = \frac{\mu}{A_0} \exp\left(\frac{s\tau^2 - 2\tau(1 - sx_a)}{2\mu}\right). \tag{58}$$

(58) matches with (55) provided that $A_0 = x_a$, which then fixes the values of the constant A_0.

We then move into region III, where from (58) $\tau - 2s^{-1}(1 - sx_a)$ is of O(1). In III we put $t = 2(s\mu)^{-1}(1 - sx_a) + \bar{t}$ and with $x = x_b + O(\mu)$ and $y = \mu Y$ we obtain the solutions which match with (58) as

$$y = \frac{\mu}{x_a} \exp\left[(1 - sx_a)\left(t - \frac{2}{s\mu}(1 - sx_a)\right)\right], \tag{59}$$

$$x = x_a + \frac{\mu}{1 - sx_a} \times \left[(1 - sx_a)t - \frac{2}{s\mu}(1 - sx_a) - s \exp\left((1 - sx_a)\left(t - \frac{2}{s\mu}(1 - sx_a)\right)\right)\right]. \tag{60}$$

Finally, to complete the cycle, the appropriate solution in region I is required. This will match to (59) and (60) and return to the initial conditions in region II. A consideration of the equations shows that this transition takes place on an O(1) time scale.

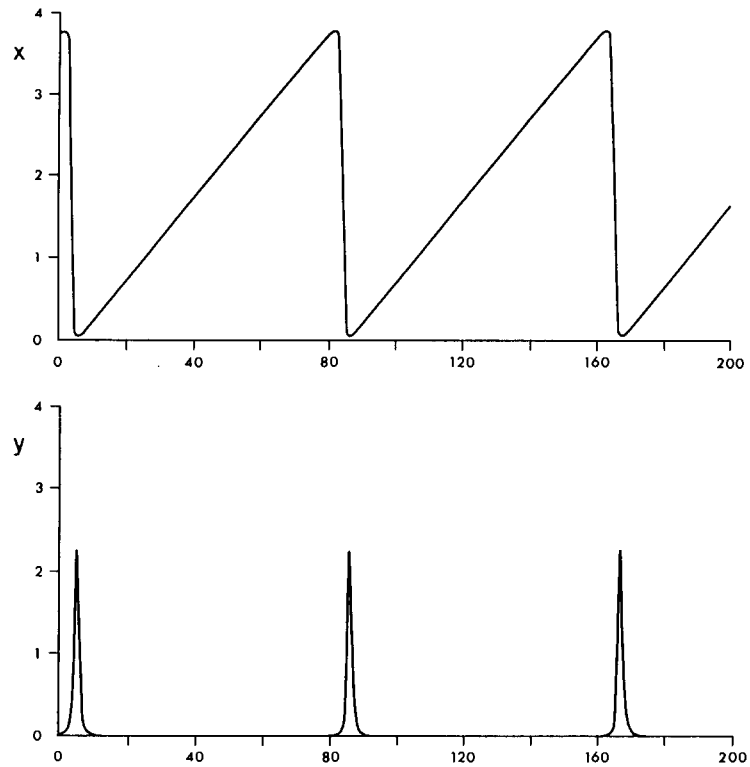

Fig. 4. Graphs of x and y against t obtained by solving equation (6) numerically for $\mu = 0.05$ and $s = 0.5$, the results are plotted from a time when the limit cycle has been reached.

The above analysis shows that at leading order the oscillatory response is given by

$$x = x_a + \mu t, \; y = 0, \qquad 0 < t < \frac{2}{\mu s}(1 - sx_a). \tag{61}$$

The discontinuity in the x waveform is smoothed out over a transition region on a time scale of O(1) with, in this transition region, y undergoing a non-zero pulse. This "saw-tooth" waveform for x and the pulse waveform for y are clearly seen in Fig. 4 where graphs of x and y obtained by integrating equations (6) numerically for a sufficiently long time so that they had settled onto the limit cycle are shown. The graphs shown in Fig. 4 are for the case $s = 0.5$ and $\mu = 0.05$. Here we can see that x rises slowly from x_a to x_b, with y being effectively zero. x then drops quickly back to x_a to restart the cycle again while y undergoes a brief excursion from zero.

From (61) the period T_p of the oscillations is given by

$$T_p = \frac{2}{s}(1 - sx_a)\mu^{-1} + \mathrm{O}(1) \tag{62}$$

and as a final check on the analysis, equations (6) were solved numerically for $s = 0.5$ and for a range of μ. From these solutions the period of the oscillations was calculated. The

Table 2. Values of the period T_p and the amplitude A_x obtained from solving equations (6) numerically for $s = 0.5$ and $r = 0$

μ	T_p	μT_p	A_x
0.10	41.16	4.116	3.5447
0.09	45.58	4.102	3.5833
0.08	51.12	4.090	3.6221
0.07	58.22	4.075	3.6612
0.06	67.74	4.064	3.7010
0.05	81.04	4.052	3.7417
0.04	100.98	4.039	3.7837
0.03	134.26	4.028	3.8276
0.02	200.82	4.016	3.8743
0.01	400.48	4.005	3.9260
0.00	∞	4.000	3.9968

results are shown in Table 2, where it is seen that, as $\mu \to 0$, μT_p is approaching a constant value as required by (62).

4. Numerical solutions

Before going on to describe the numerical solutions of equations (6) we note first that, with $r = 0$, the solution near the bifurcation point $\mu_1 = 1 - s$ can be obtained by a relatively straightforward application of the method of multiple scales [10], from which it follows that, (the details are not important and can be omitted),

$$\begin{aligned} y &= (1 - s) + (\mu_1 - \mu)^{1/2} A(T) \cos(\sqrt{1 - s}\, t + \phi) + \ldots, \\ x &= 1 - (\mu_1 - \mu)^{1/2} \frac{A(T)}{\sqrt{1 - s}} \\ &\quad \times (\sin(\sqrt{1 - s}\, t + \phi) - \sqrt{1 - s} \cos(\sqrt{1 - s}\, t + \phi)) + \ldots \end{aligned} \tag{63}$$

for $(\mu_1 - \mu) \ll 1$. The amplitude A is a function of the slow time $T = (\mu_1 - \mu)t$ and satisfies the equation

$$\frac{dA}{dT} = (1 - s)A\left(1 - \frac{1 + s}{8(1 - s)} A^2\right), \tag{64}$$

so that, as $T \to \infty$,

$$A \to \left(\frac{8(1 - s)}{1 + s}\right)^{1/2}. \tag{65}$$

As expected these expansions break down as $s \to 1$. The expansion (63) and equation (64) are the same as those given in [6] for $s = 0$, so that for s small the behaviour of the limit cycle close to bifurcation at least is not drastically altered by the inclusion of the extra autocatalytic step (5).

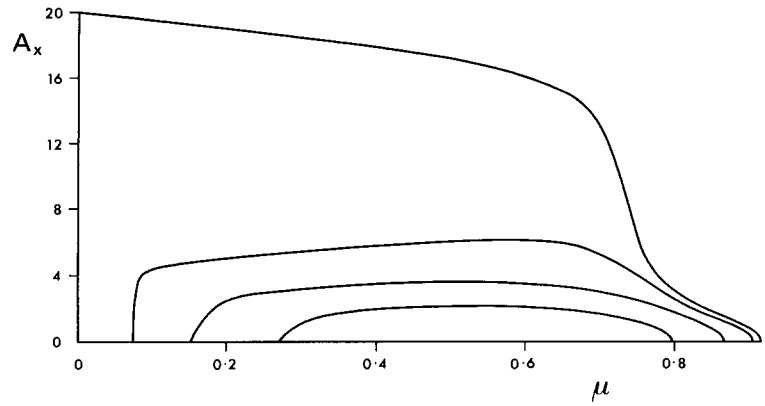

Fig. 5. Amplitude A_x plotted against μ for $s = 0.1$ with $r = 0$, $r = 0.005$, $r = 0.02$ and $r = 0.05$.

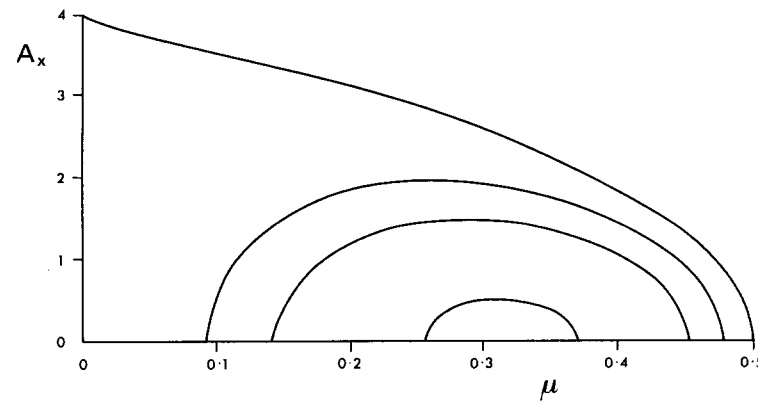

Fig. 6. Amplitude A_x plotted against μ for $s = 0.5$ with $r = 0$, $r = 0.005$, $r = 0.01$ and $r = 0.02$.

Equations (6) were integrated numerically using a Runge–Kutta method. The solution started with a perturbation to the stationary state and was continued until it had settled into a limit cycle (i.e., when the solution had repeated itself over more than 30 cycles). An integration step of 0.05 in time was generally used though this was reduced to 0.02 when more accurate information about the amplitude and period of the limit cycles was required. The number of integration steps required to reach a limit cycle depended on the values of r and s. From these solutions the amplitude $A_x = x_{\max} - x_{\min}$ was calculated and the results of two sets of integrations one with $s = 0.1$ and the other with $s = 0.5$ are shown in Figs. 5 and 6 respectively.

Consider first the case when $s = 0.1$. Here, with $r = 0$, close to bifurcation, A_x grows slowly in line with (63) and (65), it then undergoes a rapid increase around $\mu = 0.75$ before slowly approaching its final value as given by (53) as $\mu \to 0$. With $r = 0.005$ the picture is similar in that A_x still grows slowly from the first Hopf bifurcation point and undergoes a somewhat less rapid increase, but now A_x returns to zero at the second point of Hopf bifurcation.

This rapid transition in A_x is smooth though, nevertheless, can have the appearance of a bifurcation (which it is not). Such apparent bifurcations are called canards by Thompson

and Stewart [11] and here we can see that this is the remnant of the actual bifurcation at infinity in the case when $s = 0$, described in [6]. So it is interesting to see that the discontinuous behaviour for $s = 0$ survives into the case when $s \neq 0$. However, in the former case the solution then becomes unbounded, whereas in the latter it remains bounded for all $\mu > 0$. Note that there has also been a shift in the value of μ at which this canard appears from the original position of bifurcation at $\mu = 0.900\,32$.

This canard behaviour is lost when $r = 0.02$ and is not seen at all in the solutions for $s = 0.5$ (shown in Fig. 6). In this latter case A_x increases smoothly from the first Hopf bifurcation point and with $r = 0$ approaches the constant value given by (53), while with $r \neq 0$, A_x decreases smoothly to zero at the second Hopf bifurcation point.

5. Conclusions

We have considered the effect that the inclusion of both the uncatalysed and the quadratic autocatalytic reaction has on the cubic autocatalator in a closed system. These extra steps in the reaction scheme regarded as small additions to the basic scheme and, where the original scheme is stable, they give only small perturbations to the solution. However, when the basic scheme becomes unstable their effect is much more marked. In all cases oscillatory behaviour (stable limit cycles) result from a Hopf bifurcation and close to this bifurcation the behaviour (amplitude and period of the oscillations) is altered only slightly by the inclusion of these extra steps.

However, away from the bifurcation the behaviour is quite different. Without these extra steps the solution becomes unbounded, whereas with these extra steps included (no matter how small their contribution) the solution always remains bounded and oscillatory. With just the inclusion of the quadratic autocatalytic step, these oscillations persist upto the point where the model breaks down (at $\mu = 0$). While with both (or just the uncatalysed step) there is a second Hopf bifurcation point where the oscillations cease.

So we can conclude that, for a closed system, there is a range of the parameter μ for which the cubic autocatalator is structurally unstable, i.e., the nature of the solution becomes quite different on the inclusion of extra terms which can be infinitesimally small.

Acknowledgements

We wish to thank the ARGS for a Program Grant supporting M.J.R. and J.H.M. (while a visiting fellow at Macquarie University).

References

1. P. Gray and S.K. Scott, Autocatalytic reactions in the isothermal continuous stirred tank reactor: isolas and other forms of multistability, *Chem. Engng. Sci.* 39 (1983) 29–43.
2. P. Gray and S.K. Scott, Autocatalytic reactions in the continuous stirred tank reactor: oscillations and instabilities in the system A + 2B → 3B; B → C, *Chem. Engng. Sci.* 39 (1984) 1087–1097.
3. A. D'Anna, P.G. Lignola and S.K. Scott, The application of singularity theory to the isothermal autocatalytic open systems: the elementary scheme A + mB → (m + 1)B, *Proc. Roy. Soc.* A403 (1986) 341–363.

4. B.F. Gray and M. Roberts, An analysis of chemical kinetic systems over the entire parameter space: cubic autocatalysis in a c.s.t.r., to appear in *Proc. Roy. Soc.*
5. J.H. Merkin, D.J. Needham and S.K. Scott, On the structural stability of a simple pooled chemical system, *J. Engng. Math.* 21 (1987) 115–127.
6. J.H. Merkin, D.J. Needham and S.K. Scott, On the creation, growth and extinction of oscillatory solutions for a simple pooled chemical reaction scheme, *S.I.A.M. Jl. on Applied Math.* 47 (1987) 1040–1060.
7. B.F. Gray and M. Roberts, A method for the complete qualitative analysis of two coupled o.d.e.'s dependent on three parameters, *Proc. Roy. Soc.* A416 (1988) 361–389.
8. J. Guckenheimer and P. Holmes, *Nonlinear oscillations, dynamical systems and bifurcations of vector fields*, Applied Mathematical Sciences 42, Springer-Verlag (1983).
9. A.A. Andronov, E.A. Leontovich, I.I. Gordon and A.G. Maier, *Theory of dynamic systems on a plane*, Israel Program for Scientific Translations, Jerusalem (1973).
10. D.W. Jordan and P. Smith, *Nonlinear ordinary differential equations*, Oxford Applied Mathematics and Computing Science Series, Clarendon Press, Oxford (1983).
11. J.M.T. Thompson and H.B. Stewart, *Nonlinear dynamics and chaos*, John Wiley and Sons (1986).